

PACS 71.20.Mq, 78.40.Fy

The first principle calculation of electronic and optical properties of AlN, GaN and InN compounds under hydrostatic pressure

S. Berrah¹, H. Abid², A. Boukortt³

Applied materials laboratory, university of Sidi Bel Abbes, 22000 Algeria

¹E-mail: sm_berrah@yahoo.fr

²E-mail: abid_hamza@yahoo.fr

³E-mail: boukortta@yahoo.fr

Abstract. Numerical simulation based on FPLAPW calculations is applied to study the lattice parameters, bulk modulus, band energy and optical properties of the zincblende binary solids AlN, GaN, InN under hydrostatic pressure. The results obtained are in a good agreement with experimental and theoretical values.

Keywords: lattice parameter, bulk modulus, pressure coefficient, refraction index, FPLAPW, WIEN(2k).

Manuscript received 26.12.05; accepted for publication 29.03.06.

1. Introduction

The wide energy gap III-V nitride semiconductors GaN, AlN, InN and their quantum well structures have received considerable attention for their device applications in the blue and ultraviolet wavelengths [1–7]. Recently, the successful fabrication of the blue light III-V nitride semiconductor laser was first demonstrated by Nakamura [1]. The vast majority of research on III-V nitrides has been focused on the wurtzite crystal phase. The reason is that most of III-V nitrides have been grown on sapphire substrates which generally transfer their hexagonal symmetry to the nitride film. Nevertheless, interest in zincblende nitrides has been growing recently [2–6].

The zincblende GaN has a higher saturated electron drift velocity and a somewhat lower energy gap than wurtzite GaN [7].

The pressure dependence of the photoluminescence of semiconductors is very useful in understanding the electronic energy band structure and structural properties. The effect of pressure on the electronic properties of III–V compounds can be investigated experimentally in many ways [8–12]. On the other hand, both theoretical and technical developments in density functional theory (DFT) and pseudopotential calculations in recent decades have provided researchers with powerful methods for predicting electronic and energetic properties as revealed by novel experimental techniques. Meanwhile, the technical development of epitaxial growth at the end of the last century has

provided the possibility for researchers to fabricate synthetic materials with expected compositions and structures. The situation has stimulated extensive computational studies on high-pressure behavior of various semiconductors [13–17].

In this work, we carry out all-electron full-potential linearized-augmented plane waves (FPLAPW) calculation to determine band structure and optical properties of cubic binary AlN, GaN and InN under pressure within the local density approximation (LDA).

2. Calculations

Total energy calculations are performed using the FPLAPW. In this method, the unit cell is partitioned into non-overlapping muffin-tin spheres around the atomic sites and an interstitial region. In these two types of regions, different basis sets are used, the Kohn-Sham equation which is based on the DFT [18-19] is solved in a self-consistent scheme. For the exchange-correlation potential, we use the LDA ([20-21] in which the orbitals of Al ($3s^23p^1$), Ga ($3d^{10}4s^24p^1$), In ($4d^{10}5s^25p^1$) and N ($2s^22p^3$) are treated as valence electrons.

For these calculations the existing WIEN(2k) code [22] is used and applied to large unit cells. The muffin-tin radial adopted were 2.0 a.u. (Ga), 1.60 a.u. (N), 2.1 a.u. (In), and 1.8 a.u. (Al).

In the following, we use the FPLAPW method to study the bandgap and optical properties under pressure for the binary compounds of the zincblende type, GaN, AlN and InN.

3. Result and discussion

The theoretical lattice parameters and bulk modulus in this section are obtained through fitting the total energy data with the Murnaghan equation of state [23]:

$$E(V) - E(V_0) = \frac{B_0 V}{B'_0} \left[\frac{(V_0/V)^{B'_0}}{B'_0} + 1 \right] - \frac{B_0 V}{B'_0},$$

where $E(V)$ is the DFT ground-state energy with the cell volume V , V_0 is the unit-cell volume at zero pressure, B_0 denotes the bulk modulus, and their first pressure derivatives $B'_0 = \partial B / \partial p$ at $p = 0$ GPa.

The calculated structural properties (lattice parameters a , bulk modulus B_0 and B'_0) of the binaries are summarized in Table 1. We have an underestimation of the lattice parameters and an overestimation of the bulk modulus in comparison to those of experiment (Table 1), due to the use of the LDA. Table 1 shows that $B'_0 \approx 4$ for AlN, GaN and InN, which is consistent with previous results of EOS studies [24]. By the use of our calculated values of the bulk modulus B_0 , and their first pressure derivatives B'_0 , the volume change with applied pressure was calculated using the following equation [29]:

$$p = \frac{B_0}{B'_0} \left[\left(\frac{V_0}{V} \right)^{B'_0} - 1 \right].$$

The pressure dependence of E_g at the Γ , X, and L points of the energy band for the ZB phase. From the present energy band structure calculation are plotted in Figs 1, 2, and 3. Since the range of cell volume variation is $\pm 2.0\%$ for all the phases in our energy band calculations.

Table 1. The lattice parameters a , bulk modulus, and their first pressure derivative B'_0 .

		a (Å)	B_0 (GPa)	B'_0
AlN	Present work	4.353	207.85	4.186
	PWPP[25]	4.323	203.2	4.182
	Other work[26]	4.32	203	-
	Experiment	4.38 [27] 4.37 [29]	202 [28]	-
	GaN	Present work	4.475	205.38
	PWPP[25]	4.335	207	4.136
	Other work	4.446 [30]	201 [26]	-
	Experiment	4.52[27] 4.50[2]	190 [28]	-
	InN	Present work	4.949	141.16
PWPP[25]		4.801	147.6	4.06
Other work[26]		4.92	139	-
	Experiment	4.98[27]	137[28]	-

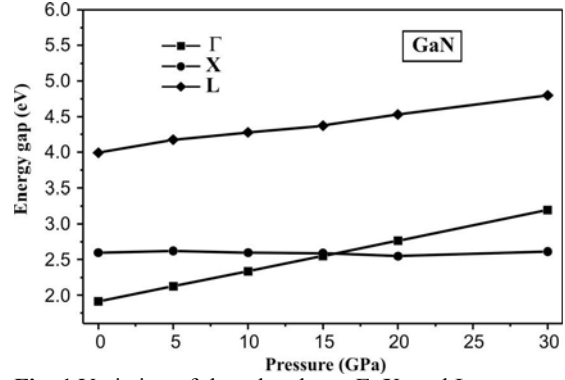


Fig. 1. Variation of three bandgaps Γ , X, and L versus pressure for GaN.

Figs 1, 2, and 3 indicate that the fundamental bandgap stays direct for InN (Fig. 2) and indirect for AlN (Fig. 3) under the pressure applied up to 21.5 GPa. In contrast, for GaN (Fig. 1), the fundamental gap becomes indirect (X) at pressure 15.53 GPa. For wurtzite GaN Zhongqin *et al.* [43] with using semiempirical tight-binding theory found that it pass from direct to indirect bandgap under 5 % strains.

In order to calculate the pressure coefficients of the fundamental bandgap, we have fitted $E_g^\Gamma(p)$ to the following linear equation: $E_g^\Gamma(p) = E_g^\Gamma(0) + k \cdot p$. Where $E_g^\Gamma(0)$ is the energy bandgap at the Γ point when $p = 0$ and is given in Table 2. k is the pressure coefficient defined by $k = E_g^\Gamma / dp$ different values for which are shown in Table 2 along with some other theoretical results.

For Γ bandgap, our calculations give $42.86 \text{ meV} \cdot \text{GPa}^{-1}$ for GaN, $19.94 \text{ meV} \cdot \text{GPa}^{-1}$ for InN, and $44.68 \text{ meV} \cdot \text{GPa}^{-1}$ for AlN. These results are in good agreement with the plane wave pseudopotential (PWPP) calculations of Kim *et al.* [25] for GaN and AlN, which gave 41.7 and $45.0 \text{ meV} \cdot \text{GPa}^{-1}$, respectively. For InN, we note that it is slightly larger than ours, namely,

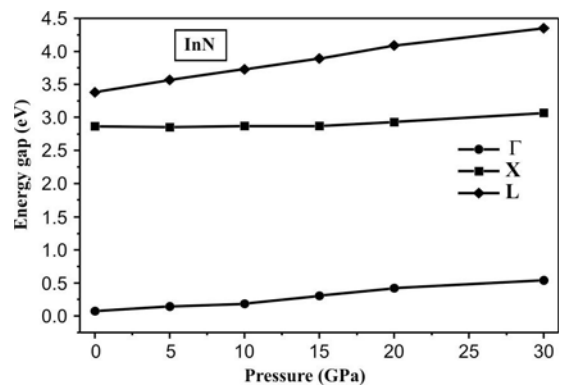


Fig. 2. Variation of three bandgaps Γ , X, and L versus pressure for InN.

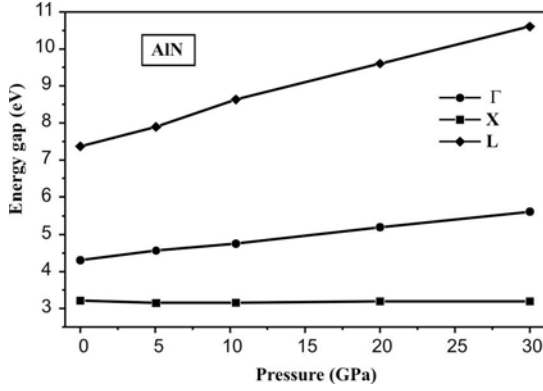


Fig. 3. Variation of three bandgaps Γ , X, and L versus pressure for AlN.

34.0 meV·GPa⁻¹. Christensen and Gorczyca [15], using LMTO calculations, have reported 42 meV·GPa⁻¹ for AlN, 40 meV·GPa⁻¹ for GaN and 16 meV·GPa⁻¹ for InN. The pseudopotential results of Van Camp *et al.* [13] for InN gave 25.4 meV·GPa⁻¹.

Table 2. Bandgap at the Γ point and pressure coefficients $k = dE_g^\Gamma / dp$ for GaN, AlN, and InN.

		E_g^Γ	k (meV·GPa ⁻¹)
AlN	Present work	4.24	44.68
	PWPP[25]	4.503	45.0
		5.94 [25]	42.0 [15]
GaN	Present work	1.80	42.86
	PWPP[25]	3.211	41.7
		3.3 [25]	40.0 [15]
InN	Present work	0.00034	19.94
	PWPP[25]	0.753	34.0
	Others		16 [15], 25.4 [13]
			0.9 [25]

4. Optical properties

We discuss now the optical properties of GaN, AlN and InN. Table 3 shows the dielectric constant $\epsilon_1(0)$, refraction index n and pressure coefficient index $d(\ln n)/dp$ in 10⁻² GPa⁻¹ for GaN, AlN, and InN in comparison with the data in the literature. We can state a quite good agreement of our data with the previously published results. Comparison of our results with previous LMTO data presented in Table 3 shows that LMTO data systematically underestimate experimental and FPLAPW results.

Fig. 4 shows the variation of the imaginary part of the electronic dielectric function ϵ_2 under normal conditions and under hydrostatic pressure for the GaN, AlN, and InN for radiation up to 15 eV. The calculated results are shifted rigidly upwards by 1.5 eV in GaN, 1.66 eV for AlN and 0.69 eV for InN. There are three groups of peaks, the first is in (3.37 – 10.58 eV) photon energy range, they are mainly due to transitions in the vicinity of M. This is usually associated with E₁ transition.

However, the L_{3v}-L_{1c} transition occurs at 8.75 eV for GaN. Similarly, the main peak in the spectra of InN and AlN is located at 6.27 and 9.56 eV, respectively. The second group of peaks is located in 10 – 12.75 eV for GaN, 7.7 – 10.04 eV for InN and 9.5 – 11.95 eV for AlN. These come from the transition L, L. The latter group of peaks is connected mainly to transitions at Γ , Γ .

The refraction index n shown in Fig. 5 was computed as a function of real dielectric function, $n = \sqrt{\epsilon_1}$ [23]. The values of the refraction index $n = \sqrt{\epsilon_1(0)}$ at low frequency are depicted in Table 3, it shown that the results occurs well with those obtained

using the Moss model [42] $n = \left(\frac{95}{E_g}\right)^{0.25}$, where E_g is the direct bandgap. With looking to the pressure coefficient index, it deduces that the refraction index decreases under pressure, and we derived also the refraction index.

Table 3. The calculated dielectric constant $\epsilon(0)$, refraction index, and pressure coefficients of the refraction index in 10⁻² GPa⁻¹ for GaN, AlN, and InN.

		$\epsilon(0)$	n	$d(\ln n)/dp$ (GPa ⁻¹)	
GaN	Present work	5.49	2.34	-0.28	
		5.30 [31]	2.3 [32]	-0.20 [15]	
		5.47 [34]	2.31[42]	-0.05 [33]	
	GGA	5.71 [35]			
		LMTO	4.68 [15]		
			5.74 [36]		
Experiment	5.7[38], 4.6[37]	2.34 [37]			
AlN	Present work	4.256	2.06	-0.31	
		4.77 [34]	1.99 [42]	-0.18 [15]	
		GGA	4.61 [35]		
	LMTO	3.86 [15]			
			4.61 [36]		
			4.46 [39]		
Experiment	4.68 [40]				
InN	Present work	8.56	2.92	-2.60	
		8.4 [34]	3.20 [42]	-0.43 [15]	
		GGA	7.46 [35]		
	LMTO	7.16 [15]			
		Experiment	8.40 [41]		

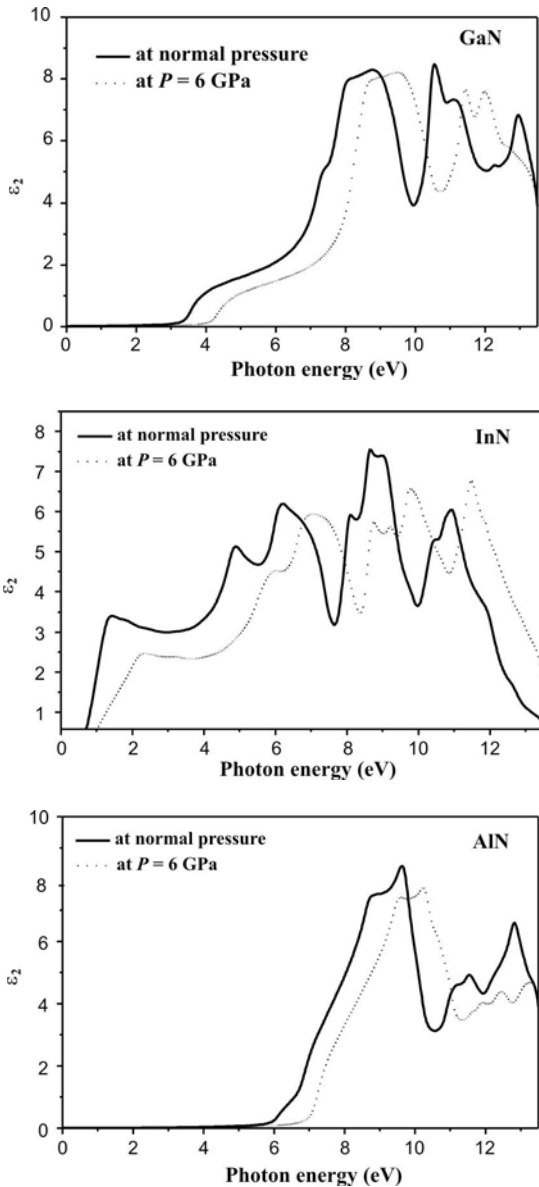


Fig. 4. Imaginary part of the dielectric function of GaN, InN, and AlN under normal conditions and under pressure.

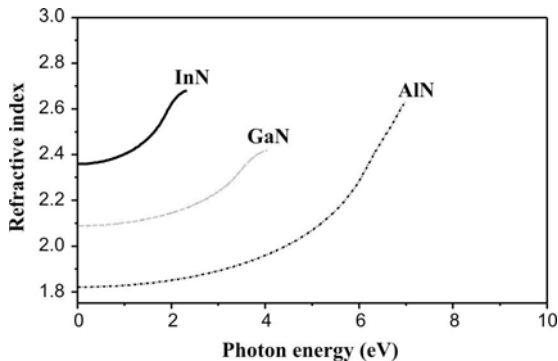


Fig. 5. Refraction index of GaN, AlN, and InN.

5. Conclusions

In this work, we have reported the band structure and optical properties of zincblende GaN, AlN and InN under pressure with using FPLAPW method within LDA.

It was shown that for AlN and InN, the fundamental bandgap increases and stays direct with pressure, while for GaN, the fundamental bandgap becomes indirect (Γ -X) at $p = 15.53$ GPa. So, in the view of fabrication of blue emitting-light devices, it is necessary to try to decrease strains.

However, the pressure coefficient of the fundamental gap obtained are in a good agreements with others.

The optical properties of zincblende nitrides have been also investigated under normal conditions and under hydrostatic pressure. It is shown that the refraction index decreases under pressure. Our value $d(\ln n)/dp = -0.28 \cdot 10^{-2} \text{ GPa}^{-1}$ for GaN, $-0.31 \cdot 10^{-2} \text{ GPa}^{-1}$ for AlN and $-2.6 \cdot 10^{-2} \text{ GPa}^{-1}$ for InN obtained from the calculated $\epsilon_1(0)$. They are in an excellent agreement with the experimental value, $-0.19 \cdot 10^{-2} \text{ GPa}^{-1}$ for GaN, -0.18 for AlN and -0.43 for InN [15].

Acknowledgements

We would like to acknowledge S.Q. Wang from Shenyang National Laboratory for Materials Science, Institute of Metal Research, Chinese (republic of China) and K. Louzazna from university of Béjaia (Algéria) for their help.

References

1. S. Nakamura, M. Senoh, S. Nagahma, N. Iwasa, T. Yamada, T. Matsuahita, H. Kiyoku, and Y. Sugimoto // *Jpn J. Appl. Phys.* **35**, p. 174 (1996).
2. T. Lei, T.D. Moustakas, R.J. Graham, Y. He, and S.J. Berkowitz // *J. Appl. Phys.* **71**, p. 4933 (1992).
3. S.J. Hwang, W. Shan, R.J. Hauenstein, and J.J. Song // *Appl. Phys. Lett.* **64**, p. 2928 (1994).
4. A. Rubio, J.L. Corkill, M.L. Cohen, E.L. Shirley, and S.G. Louie // *Phys. Rev.* **B 48**, 11810 (1993).
5. E.A. Albanesi, W.R.L. Lambrecht, and B. Segall // *Phys. Rev.* **B 48**, 17841(1993).
6. A.F. Wright and J.S. Nelson // *Phys. Rev.* **B 50**, p. 2159 (1994).
7. S. Strite and H. Morkoc // *J. Vac. Sci. Technol.* **B 10**, p. 1237 (1992).
8. H. Muller, R. Trommer, M. Cardona and P. Vogl // *Phys. Rev.* **B 21**, p. 4879 (1980).
9. C. Menoni, H. Hochheimer, and I. Spain // *Phys. Rev.* **B 33**, p. 5896 (1986).
10. R. Zallen and W. Paul // *Phys. Rev.* **155**, p. 703 (1967).
11. G. Pitt // *J. Phys. C: Solid State Phys.* **6**, p. 1586 (1973).

12. Y. Vohra, S.T. Weir, and A.L. Ruoff // *Phys. Rev. B* **31**, p. 7344 (1985).
13. P.E. Van Camp, V.E. Van Doren and J.T. Devreese // *Phys. Rev. B* **41**, p. 1598 (1990).
14. K. Kim, W.R.L. Lambrecht, and B. Segall // *Phys. Rev. B* **50**, p. 1502 (1994).
15. N.E. Christensen and I. Gorczyca // *Phys. Rev. B* **50**, p. 4397 (1994).
16. A.A. Kelsey and G.J. Ackland // *J. Phys.: Condens. Matter* **12**, p. 7161 (2000).
17. M.H. Tsai, J.D. Dow and R.V. Kasowski // *J. Mater. Res.* **7**, p. 2205 (1996).
18. P. Hohenberg and W. Kohn // *Phys. Rev.* **136**, No 3B, p. 864 (1964).
19. W. Kohn and L.J. Sham // *Ibid.* **140**, No 4A, p. 1133 (1965).
20. G. Ortiw // *Phys. Rev. B* **45**, 11328 (1992).
21. C. Browe, G. Sugiyama, and B.J. Alder // *Phys. Rev. B* **50**, 14838 (1994).
22. P. Blaha, K. Schwarz, G.K.H. Madsen, D. Kvasnicka, J. Luitz, WIEN2k, *An augmented plane wave plus local orbitals program for calculating crystal properties*. Vienne University of Technology, Vienna, Austria, 2001.
23. F.D. Murnaghan // *Proc. Nat. Acad. Sci. USA* **30**, p. 244 (1944).
24. R. Jeanloz // *Phys. Rev. B* **38**, p. 805 (1988).
25. S.Q. Wang and H.Q. Ye // *J. Phys.: Condens. Matter* **14**, p. 9579–9587 (2002).
26. K. Kim, W.R.L. Lambrecht, and B. Segall // *Phys. Rev. B* **53**, 16 310 (1996).
27. A. Trampert, O. Brandt, and K.H. Ploog, in: Crystal structure of group III nitrides, edited by J.I. Pankove and T.D. Moustakas, *Semiconductors and semimetals*, Vol. 50. Academic, San Diego, 1998.
28. M.E. Sherwin and T.J. Drummond // *J. Appl. Phys.* **69**, p. 8423 (1991).
29. J.H. Edgar, *Properties of group III nitrides (Electronic Materials Information Service (EMIS), Data reviews series)*. Institution of Electrical Engineers, London, 1994.
30. S. Logothetidis, J. Petalas, M. Cardona and T.D. Moustakas // *Phys. Rev. B* **50** 18 017 (1994).
31. R. Goldhan, S. Shokhovets, in: *III-nitride semiconductors optical properties II*, M.O. Mansrejm H.X. Jiang, editors, Taylors and Francis, p. 7363, 2002.
32. H. Harima // *J. Phys.: Condensed Matter* **14**, p. R967-R993 (2002).
33. D.L. Camphausen, G.A. Neville Conell and W. Paul // *Phys. Rev. Lett.* **26**, p. 184 (1971).
34. V.W.L. Chin, T.L. Tansley, and T. Osotchan // *J. Appl. Phys.* **75**, p. 7365-7372 (1994).
35. V.I. Gavrilenko and R.Q. Wu // *Phys. Rev. B* **61**, p. 2632 (2000).
36. J. Chen, Z.H. Levine, and J.W. Wilkins // *Appl. Phys. Lett.* **66**, p. 1129 (1995).
37. U. Köhler, D.J. As, B. Schöttker, T. Frey, K. Lischka, J. Scheiner, S. Shokhovets, and R. Goldhahn // *J. Appl. Phys.* **85**, p. 404 (1999).
38. P. Perlin, I. Gorczyca, N. E. Christensen, I. Grzegory, H. Teisseyre, and T. Suski // *Phys. Rev. B* **45**, 13 307 (1992).
39. K. Karch and F. Bechstedt // *Phys. Rev. B* **56**, p. 7404 (1997).
40. L. Akasaki and M. Hashimoto // *Solid State Commun* **5**, 851 (1967).
41. J. Misek and F. Srobar // *Phys. Rev. B* **61**, P. 6720 (2000).
42. T.S. Moss // *Proc. Phys. Soc.* **B 63**, 167 (1950).
43. Y. Zhongqin, X. Zhizhong // *Phys. Rev. B* **54**, 17 577 (1996).